Food Chemistry 437 (2024) 137726

Contents lists available at ScienceDirect

Food Chemistry

journal homepage: www.elsevier.com/locate/foodchem

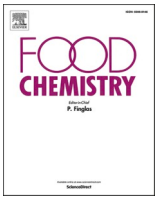

Exploring UPLC-QTOF-MS-based targeted and untargeted approaches for understanding wine mouthfeel: A sensometabolomic approach

Sara Ferrero-del-Teso [a], Panagiotis Arapitsas [b,c], David W. Jeffery [d], Chelo Ferreira [e], Fulvio Mattivi [b], Purificación Fernández-Zurbano [a], María-Pilar Sáenz-Navajas [a,*]

[a] Instituto de Ciencias de la Vid y del Vino (Universidad de La Rioja-Consejo Superior de Investigaciones Científicas-Gobierno de La Rioja), Departamento de Enología, Logroño, La Rioja, Spain
[b] Unit of Metabolomics, Research and Innovation Centre, Fondazione Edmund Mach, via E. Mach 1, 38010 San Michele all'Adige, Italy
[c] Department of Wine, Vine and Beverage Sciences, School of Food Science, University of West Attica, Ag. Spyridonos 28, Egaleo, 12243 Athens, Greece
[d] School of Agriculture, Food and Wine, and Waite Research Institute, The University of Adelaide, PMB 1, Glen Osmond, South Australia 5064, Australia
[e] Laboratorio de Análisis del Aroma y Enología (LAAE), Instituto Universitario de Matemáticas y Aplicaciones (IUMA-UNIZAR), Universidad de Zaragoza, c/ Pedro Cerbuna 12, 50009 Zaragoza, Spain

ARTICLE INFO

Keywords:
Sensory analysis
High-resolution MS
PLS regression
Drying
Astringency
Anthocyanins
Amino acids
Peptides

ABSTRACT

This study aimed to establish relationships between wine composition and in-mouth sensory properties using a sensometabolomic approach. Forty-two red wines were sensorially assessed and chemically characterised using UPLC-QTOF-MS for targeted and untargeted analyses. Suitable partial least squares regression models were obtained for "dry", "sour", "oily", "prickly", and "unctuous". "Dry" was positively contributed by flavan-3-ols, anthocyanin derivatives (AntD), valine, gallic acid and its ethyl ester, and peptides, and negatively by sulfonated flavan-3-ols, anthocyanin-ethyl-flavan-3-ols, tartaric acid, flavonols (FOL), hydroxycinnamic acids (HA), protocatechuic ethyl ester, and proline. The "sour" model included molecules involved in "dry" and "bitter", ostensibly as a result of cognitive interactions. Derivatives of FOLs, epicatechin gallate, and *N*-acetyl-glucosamine phosphate contributed positively to "oily", as did vanillic acid, HAs, pyranoanthocyanins, and malvidin-flavan-3-ol derivatives for "prickly", and sugars, glutathione disulfide, AntD, FOL, and one HA for "unctuous". The presented approach offers an interesting tool for deciphering the sensory-active compounds involved in mouthfeel perception.

1. Introduction

The perceived intrinsic quality of red wines is initially judged by colour. It can be further defined by the absence of volatile molecules capable of depreciating aroma quality, whether at supra or subthreshold levels (de-la-Fuente-Blanco et al., 2017), either because they provide unpleasant aromas or are able to mask the positive ones (Ferreira et al., 2009). In the presence of desirable odorant molecules that contribute a positive valence, wine palate properties (taste and mouthfeel) will then play a key role in defining the quality of a wine (Gawel et al., 2000; Jones et al., 2008; Sherman et al., 2020). Notably, taste and mouthfeel properties of wines can be considerably affected by climate change, which leads to modifications in both the overall sensory profile of wines and the underlying polyphenolic content, culminating in the perception of undesirable palate sensations (Sáenz-Navajas et al., 2018).

Despite the importance of taste and mouthfeel properties in modulating wine quality and consumer acceptance, the specific chemical markers are practically unknown and limited knowledge can be found in the scientific literature. In this regard, Fig. 1 provides a graphical summary of the main topics dealing with "wine", "mouthfeel", and "composition" obtained from the Web of Science database over the past decade. Six main clusters of research topics appear, including "phenolic composition" (in red), which captures the highest frequency of occurrence among all the published research. This is directly linked to the second cluster (in violet) dealing with publications related to "fermentation", namely "yeasts", "strains" and "saccharomyces cerevisiae" as well as to the third cluster (in dark blue) dealing with "vintage" and "season", and to a lesser extent to "vine" and "total phenolic content".

Abbreviations: **CATA**, check-all-that-apply; ***epi*-DPA-G**, *epi*-dihydrophaseic-3′-O-β-glucopyranoside acid; **tCATA**, temporal check-all-that-apply.

* Corresponding author.
E-mail address: mpsaenz@icvv.es (M.-P. Sáenz-Navajas).

https://doi.org/10.1016/j.foodchem.2023.137726
Received 16 February 2023; Received in revised form 13 September 2023; Accepted 8 October 2023
Available online 11 October 2023

The fourth cluster (in light blue) reveals research associated with "consumer" and "panelist", including sensory and sensometric approaches such as "CATA", "tCATA", "trained panel" or "principal component analysis". This cluster, mainly devoted to perception, is closely related to the fifth (in yellow) and sixth (in green) clusters. The yellow cluster deals with the sensory percepts "bitter taste" and "dryness" and relates to chemical composition in terms of "proanthocyanidins", "organic acid", "tannin activity", "persistence" and "phenolic compounds", which also link with cluster 1. Finally, the sixth cluster (in green) relates to additional mouthfeel dimensions associated with "body" or "viscosity" that can be explained in terms of wine composition involving "protein", "glucose", "polysaccharide", "glycerol" or "ethanol", although these have mainly been studied in white wines (Gawel et al., 2013).

This literature analysis highlights that phenolic composition is the topic capturing the highest attention, but such chemical information is scarcely related to sensory percepts (i.e., lower frequency of occurrence and thus smaller size of sensory-related words), and mostly limited to perceptions of wine bitterness and drying (García-Estévez et al., 2017; García-Estévez et al., 2018). Thus, the scientific literature aimed at establishing relationships between taste and mouthfeel properties and chemical composition is mostly focused on explaining astringency, and to a lesser extent bitterness, from phenolic content and/or phenolic structure-related measurements following different strategies.

Most extended approaches dealing with both sensory and chemical information have certain limitations. Regarding sensory approaches, it should be considered that wine mouthfeel involves multiple sensations resulting in a multidimensional percept that includes various subqualities. Even though "astringency" is the most studied mouthfeel attribute in red wines, there are other sensory dimensions that must be considered to fully understand wine mouthfeel (Ferrero-del-Teso et al., 2022; Gawel et al., 2000; Kang et al., 2019; Rinaldi et al., 2021; Sáenz-Navajas et al., 2017). Regarding analytical approaches, targeted liquid chromatography (LC) coupled to UV–Vis or mass spectrometric detectors (Ma et al., 2014) is among the most used. However, one disadvantage is that classical targeted LC quantification does not make full use of an abundance of chemical information, as only compounds with available standards, known sensory activity, or sufficient concentration are analysed.

The issue with targeted LC analysis has been evidenced when modelling wine mouthfeel properties from chemical composition, where tannin activity was shown to be a good predictor of wine dryness/silky on the palate, and tannin concentration could model both "dry" (in general) and "dry on the palate" attributes. However, the results highlighted that the other independent mouthfeel dimensions could not be linked to the chemical variables studied (Sáenz-Navajas et al., 2020). Similarly, applying a targeted instrumental approach to understand the mouthfeel properties elicited by grape fractions, tannin activity, and tannin concentration along with mean degree of polymerisation (mDP) of tannins proved to be good for predicting perceived dryness (Ferrero-del-Teso et al., 2022). In addition, low molecular weight anthocyanins seemed to be involved in the formation of the "dry" attribute, whereas large polymeric pigments were related to the "sticky" dimension. Distinctly, the "coarse" dimension could not be modelled, which

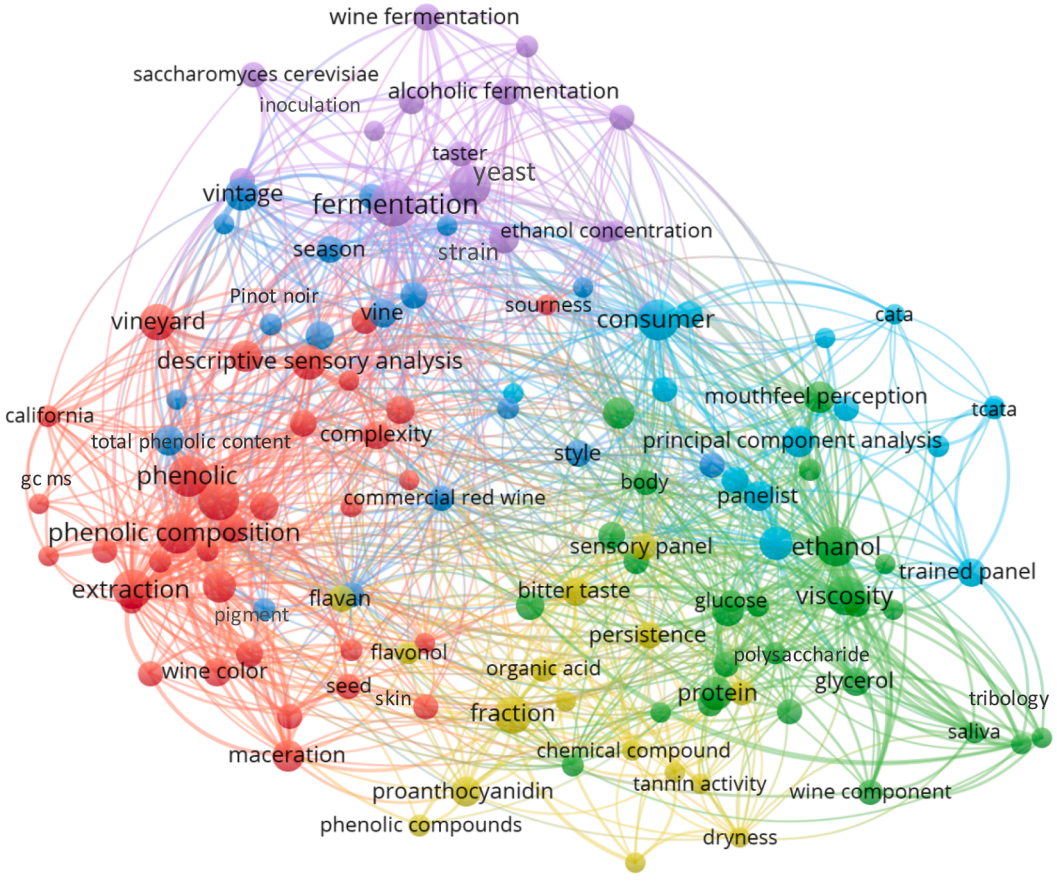

Fig. 1. Bibliometric network diagram arising from a search involving "wine", "mouthfeel", and "analysis" using Web of Science Core Collection within the last 10 years. Different colours are used to indicate to which of the six clusters a term belongs. Each cluster is mainly characterised by the following terms (i.e., highest citation within a given cluster): 1) "phenolic composition" (in red), "fermentation" (in violet), "vintage" and "season" (in dark blue), "consumer" (in light blue), "bitter taste" (in yellow), and "viscosity" and "ethanol" (in green). Generated with VOSviewer version 1.6.18 using the default settings for both the minimum number of occurrences of a term and the number of terms to be selected. Note that not all terms are labelled in the figure to facilitate interpretation.

suggests that there are other molecules involved in the formation of this percept that are not measured by targeted LC (Ferrero-del-Teso et al., 2022). Essentially, targeted approaches neglect the importance of unknown metabolites (Vallverdú-Queralt et al., 2017) as well as those present at low concentrations, which could nonetheless play a major role in the formation of taste and mouthfeel properties (Aydoğan, 2020; Sherman et al., 2020).

Development of LC with high-resolution mass spectrometry (HRMS) in the last decade has revolutionised the study of food and natural product chemistry (Aydoğan, 2020; Cevallos-Cevallos & Reyes-De-Corcuera, 2012). The application of untargeted analytical methods is powerful and provides a promising alternative tool to targeted methods for identifying chemical markers involved in different chemical and biological phenomena, and for characterising the metabolome of a given system (Kueger et al., 2012; Sherman et al., 2020; Vallverdú-Queralt et al., 2017). Regarding the profiling of wine metabolome, however, untargeted approaches have been scarcely used to explore relationships between chemical composition and sensory properties, being limited to some recent contributions dealing with volatile composition (Chávez-Márquez et al., 2022) or considering both volatile and non-volatile fractions to predict perceived quality of Pinot Noir wines (Sherman et al., 2020) or the sensory properties of rosé wines (Muñoz-Redondo et al., 2021).

In spite of the potential for using metabolomics to help unravel the sensory activity of compounds, sensomics as defined by Toelstede and Hofmann (2008) has not yet been explored to elucidate drivers of sensations experienced on the palate and predict wine taste and mouthfeel properties from wine composition. In this context, and with the need to explore new analytical approaches for understanding the chemical basis of mouthfeel, the goal of this work was to employ a sensomic approach to establish relationships between red wine composition and mouthfeel properties, considering the wine metabolome holistically using a UPLC-QTOF MS approach. More specifically, the main objectives of this study were: (1) to identify molecular markers of the mouthfeel dimensions following an untargeted metabolomic approach, and (2) to generate mathematical models able to predict mouthfeel dimensions from non-volatile chemical markers identified by both untargeted and targeted methods that provide more complete information. The hypothesis behind this project is that the untargeted UPLC-QTOF MS approach will enrich the information regarding sensory active molecules involved in wine mouthfeel perception by enabling the prediction of other dimensions differing from those modelled by targeted UPLC-QTOF MS approaches.

2. Material and methods

2.1. Chemicals

LC-MS grade methanol and formic acid used for the preparation of mobile phase were purchased from Sigma-Aldrich (St Louis, MO). Water for chromatography was purified by a Milli-Q system (Millipore, Molsheim, France).

2.2. Wine samples

Unwooded monovarietal wines (n = 42) selected in previous work (Sáenz-Navajas et al., 2020) were studied. Wines covered 14 different varieties from different origins (Spain, Argentina, and France) and vintages (2014–2018). The sample set included commercial and non-commercial red wines. A detailed list of wine characteristics is presented in Table A.1 of Appendix A.

Reducing sugars, ethanol content, pH, and titratable acidity were analysed using Fourier transform infrared spectroscopy with a WineScan FT 120 (FOSS, Barcelona, Spain) calibrated against official OIV reference methods (OIV, 2021). Wines were analysed immediately upon opening without centrifugation, acquiring duplicate infrared spectra for each sample. Total polyphenol index (TPI) was estimated from absorbance at 280 nm (Ribéreau-Gayon, 1970) using 1-cm quartz cuvettes and a Shimadzu UV-1800 spectrophotometer (Kyoto, Japan). Wines for TPI analysis were filtered (0.45 μm) and diluted 100-fold with deionised water to obtain absorbance values in the range of 0.2–0.9.

2.3. Sensory characterisation

The sensory data derived from the mouthfeel characterisation of wines using nose clips as described elsewhere (Sáenz-Navajas et al., 2020) were considered in the present work. Briefly, sensory analysis was carried out by 18 wine experts from the Rioja area of Spain. The list of terms employed in the rate-k-attributes (k = 5) sensory strategy (i.e., a variant of rate-all-that-apply) consisted of 23 taste and mouthfeel-related attributes (Sáenz-Navajas et al., 2017) (Table A.2 of Appendix A). Participants were asked to taste samples and rate the intensity of a maximum of five attributes appearing in each sample on a 7-point scale (1 = not intense; 7 = very intense).

2.4. Ultra-performance liquid chromatography – quadrupole time-of-flight mass spectrometry (UPLC – QTOF-MS) analysis

2.4.1. Sample preparation

One mL of each wine sample was diluted with 2 mL of sonicated (Falc Instruments, Italy) Milli-Q water, and filtered with Millex® syringe driven filter discs (0.22 μm, PTFE, Merck Millipore Ltd, Tullagreen, Ireland) into a 2 mL vial for analysis. A quality control (QC) sample was prepared by pooling 1 mL of each of the 42 wines, prior to dilution and filtration as specified above. The samples were prepared and analysed according to a randomised order (https://www.random.org/sequences/). At the beginning of each batch, one blank sample (Milli-Q water) and five QC samples were analysed, followed by wine samples, with one QC after every six samples. At the end of each batch, one QC and one blank were injected.

2.4.2. UPLC system

The liquid chromatography system was a Waters Acquity UPLC coupled via an electrospray ionisation (ESI) interface to a Synapt HDMS QTOF-MS (Waters, Manchester, U.K.) operating in W mode and controlled by MassLynx 4.1 software. Separation was performed with an Acquity UPLC HSS T3 column (2.1 × 150 mm, 1.8 μm, Waters) at 40 °C with an injection volume of 10 μL. Samples were maintained at 4 °C in the autosampler prior to injection.

The LC – MS conditions were in accordance with the method described in Arapitsas et al. (2014) and used by Arapitsas et al. (2016). Briefly, mobile phase flow rate was 0.28 mL/min and the eluents were water (A) and methanol (B), both containing 0.1 % v/v formic acid with the following gradient: 0–1 min, 0 % B; 1–3 min, 10 % B; 3–18 min, 40 % B; 18–21 min, 100 % B; 21–25.5 min, 100 % B; 25.5–25.6 min, 0 % B; 25.6–28 min, 0 % B.

Mass spectral data (full scan and W mode) were collected in positive and negative ESI modes during separate runs over a mass range of 50–2000 Da with scan duration of 0.4 s in centroid mode. The transfer collision and trap collision voltages were set at 6 and 4 V, respectively. The source parameters were set as follows: capillary, 3 kV for positive mode and 2.5 kV for negative; sampling cone, 25 V; extraction cone, 3 V; source temperature, 150 °C; desolvation temperature, 500 °C; desolvation gas (N_2) flow, 1000 L/h; and nebuliser gas (N_2), 50 L/h.

External calibration of the instrument was performed at the beginning of each batch of samples by direct infusion of a sodium formate solution (10 % formic acid/0.1 M NaOH/acetonitrile at a ratio of 1:1:8), controlling the mass accuracy from *m/z* 40 to 2000 (less than 5 ppm), and mass resolution (>14,000 FWHM) in W-optics mode. LockMass calibration was applied using a solution of leucine enkephalin (0.5 mg/L, *m/z* 556.2771 for positive ion mode and 554.2620 for negative) at 0.1 mL/min.

2.4.3. MS/MS conditions

For unknown features to be further identified, MS/MS data were acquired in V-optics mode (>5,000 FWHM resolution) in order to increase sensitivity; the data were acquired in centroid mode with a scan duration of between 0.2 and 0.5 s. For MS/MS experiments, the molecular ions were fragmented by setting the transfer collision energy to 20 and 40 eV.

Targeted and untargeted analyses were carried out following similar UPLC–MS/MS conditions. In the targeted approach, 108 known compounds (Table A.3 of Appendix A) were identified based on analytical standards and their area was acquired for data analysis. For the untargeted approach, features were selected based on sensory data as explained in the data analysis section.

2.5. Data analysis

2.5.1. Sensory analysis: Rate-k-attributes

The data derived from the sensory description collected in Sáenz-Navajas et al. (2020) were firstly submitted to two-way ANOVA (panellists as random factor and samples as fixed) for each of the 23 attributes of the list. Attributes that were not rated were allocated a value of zero when collecting data. Principal component analysis (PCA) was carried out with the correlation matrix of mean intensity scores (n = 18 judges) for significant attributes. Significant PCs were considered according to Kaiser criterion (eigenvalue ≥ 1). Hierarchical cluster analysis (HCA) with the Ward criteria was applied to all dimensions derived from PCA. To identify the attributes that best defined clusters, two-way ANOVA with the scores of attributes was calculated with panellists as the random factor and cluster as the fixed factor. Similarly, for conventional oenological parameters, one-way ANOVA was calculated considering sensory clusters as fixed factor. For significant attributes ($P < 0.05$), Fischer pair-wise comparison test was applied ($\alpha = 0.05$). All analyses were carried out with XLSTAT (version 2019.3.1.60623).

2.5.2. UPLC − QTOF-MS analysis

For quality control purposes and to guarantee the robustness of the data during the untargeted runs and upon data analysis, PCA plots generated by Progenesis QI (version 2.4, nonlinear dynamics) were calculated for each ionisation mode. The raw files were imported directly into the software and the distribution/clustering of the QC injections was checked (Arapitsas et al., 2018).

Default Progenesis QI parameters were used for alignment, with peak picking performed at the maximum level, and the first minute and last 6 min of the run excluded from data processing (i.e., data from 1 − 22 min were used). By default, the software considers a group of isotopic and adduct features coming from the same metabolite as a "compound". Presumed markers/features were considered the "compounds" that, according to the Progenesis QI statistical analysis, had a maximum fold range of ≥ 2 and were significant according to ANOVA ($P \leq 0.05$), considering the clusters derived from sensory description as fixed factors. The pattern of the selected features was visually inspected one by one. Therefore, for each feature, significant differences of the area between the two clusters were visually confirmed with Progenesis QI tool. Subsequently, a semi-manual integration of visually inspected "putative markers" was performed using the TargetedLynx tool of MassLynx 4.1 software. Finally, in order to filter "putative markers", Pearson correlation coefficients were calculated between sensory scores and semi-quantitative data (peak area).

Feature annotation was performed manually by comparing retention time and mass spectra accuracy with a mass tolerance of 5 ppm, based on the previous experience of the group with the specific instrumentation mass resolution and in accordance with the four levels of annotation described by Sumner et al. (2007). Those levels correspond to: (1) identified compounds; (2) putatively annotated; (3) putatively characterised compound classes, and (4) unknown. MS/MS data was also registered to support the annotation of selected tentative biomarkers.

The targeted approach was based on the internal standard data set of the laboratory of Food Quality and Nutrition Department at Fondazione Edmund Mach (FEM) (chromatographic and spectral libraries of over 400 compounds obtained in the same condition of the experiment). With this approach it was possible to tentatively identify well-known wine metabolites previously annotated using the same protocol and therefore under the same conditions of the experiment (i.e., targeted compounds). The annotated wine metabolites were integrated using the TargetedLynx tools of Waters MassLynx 4.1 software (Milford, MA, U.S.A.). The parameters of the integration were set at chromatogram mass window of 0.08 Da, retention time window of ± 0.2 min, smoothing iterations of 1, and smoothing width of 2.

2.5.3. PLS regression modelling

Regression models were calculated to predict sensory variables from chemical compounds (i.e., tentative chemical markers and targeted compounds) identified following the two approaches indicated above (i.e., untargeted and targeted).

The mathematical prediction model for each one of the sensory attributes is given by:

$$Y = XB + F$$

where, for a sample size n ($n = 42$), $X_{(42,61)}$ for untargeted and $X_{(42,108)}$ for targeted represent the input matrix, $Y_{(42,1)}$ is the output matrix for the sensory variable, $B_{(61,1)}$ and $B_{(108,1)}$ are the matrix of regression coefficients, and $F_{(42,1)}$ the matrix of residuals (different residuals depending on the input targeted or untargeted matrix). The model is computed by PLS1 regression.

Input variables X were standardised to comparable noise levels (i.e., z-scores were calculated). Likewise, sensory variables Y were also standardised.

With these considerations, a first PLS model was computed. Models were validated using k-fold cross-validation procedure with $k = 10$. Then, those models with validated explained variance greater than 39 % were considered (i.e., regression coefficient, $r > 0.6$). The number of factors (i.e., latent variables, LVs) retained for each model accorded with the maximal explained predicted variance with the minimal number of factors and minimal root means square error for calibration (RMSEC) and validation (RMSECV).

The analyses were carried out with Unscrambler X 10.5.1, Matlab R2018a, R 4.0, and XLSTAT (version 2019.3.1.60623).

3. Results and discussion

3.1. Sensory characterisation of wines

Two-way ANOVA calculated with sensory data collected in Sáenz-Navajas et al. (2020) yielded eight significantly ($P < 0.05$) attributes and a tendency for other four attributes among the 23 that were evaluated (Table A.4 of Appendix A). The eight significant attributes were "bitter", "sweet", "dry", "dry on tongue side", "dry on palate", "unctuous", "oily", and "watery"; another four attributes ("sour", "silky", "burning" and "prickly") were considered when relaxing the criteria for significance ($P < 0.1$). The PCA calculated with the average scores of these 12 attributes yielded four independent and non-correlated sensory dimensions, explaining 71 % of the original variance and of significance according to the Kaiser criterion (Fig. A.1 of Appendix A). The first PC (31.43 % explained variance, Fig. A.1a) was positively contributed by the terms "dry on palate" ($r = 0.80$), "dry" ($r = 0.80$), and "bitter" ($r = 0.57$), and negatively by "silky" ($r = -0.72$) and "unctuous" ($r = -0.66$). The second PC (18.90 % of explained variance, Fig. A.1a) was positively contributed by "oily" ($r = 0.70$) and negatively by "sour" taste ($r = -0.66$). The third dimension (11.26 % explained variance, Fig. A.1b) was mainly influenced positively by "sweet" taste ($r = 0.79$) and negatively by "burning" ($r = -0.61$). Finally, the fourth PC (8.95 % of explained variance, Fig. A.1b) was positively contributed by "dry on tongue" ($r = 0.63$) and negatively by "prickly" ($r = -0.60$). The PCA result confirms

the sensory variability in terms of mouthfeel properties of the sample set. The first dimension is linked to different levels of dryness, often referred to by the global term "astringency". Besides this commonly studied percept, the use of this sensory approach together with the relatively high number of wines employed highlights the presence of another three dimensions explaining mouthfeel variability and related to "oily", "burning", and "dry on the tongue"/"prickling" sensations. The identification of these four independent mouthfeel dimensions may indicate an advantage of the RATA-based methodology compared to other sensory approaches that usually lead to high correlations among terms (Wang et al., 2021) and that can limit the identification and interpretation of other attributes contributing to wine mouthfeel variability.

Having confirmed the mouthfeel variability among the sample set, salient sensory differences among the wines in terms of mouthfeel perception were identified by HCA calculated on all the PCA dimensions. The result highlighted the presence of two main clusters of wines formed by 23 (Cluster 1) and 19 (Cluster 2) samples (Fig. 2). ANOVA results showed 10 significant attributes differing among clusters ("sweet" and "burning" were not significantly different). Cluster 1 presented significantly higher scores than Cluster 2 for the terms "dry on palate" ($F = 37.98$; $P < 0.001$), "dry" ($F = 35.06$; $P < 0.001$), "dry on tongue" ($F = 13.66$; $P < 0.01$), and "bitter" ($F = 12.71$; $P < 0.01$), whereas Cluster 2 presented higher scores than Cluster 1 for the terms "silky" ($F = 23.03$; $P < 0.001$), "sour" ($F = 20.11$; $P < 0.01$), "watery" ($F = 17.81$; $P < 0.01$), "unctuous" ($F = 8.91$; $P < 0.01$), "oily" ($F = 4.71$; $P < 0.05$), and "prickly" ($F = 4.11$; $P < 0.05$). The clustering of wines into two main differentiated groups facilitated the selection of chemical features that could be used to understand the mouthfeel differences.

ANOVA calculated with conventional oenological parameters in Table 1 showed that exclusively, total polyphenol index was significantly ($F = 6.90$; $P < 0.05$) higher in Cluster 1 than in Cluster 2. This result is well in line with the significant correlation found in red wines between TPI and the descriptors "dry" and "dry on palate" (Sáenz-Navajas et al., 2020). Besides, the results accorded with the presence of varieties rich in polyphenols such as Bobal, Cabernet Sauvignon (4 samples out of 5), and Merlot (3 out of 4) in Cluster 1, whereas the two Pinot Noirs studied appeared in Cluster 2. The remaining varieties in the sample set (i.e., Tempranillo Tinto, Syrah, Mencia, Gamay, Bornarda, Garnacha Tinta, and Prieto Picudo) showed high variability and were distributed in both clusters.

Table 1
Range of occurrence and median values of conventional oenological parameters of the 42 wines studied. Significance (P) for one-way ANOVA calculated considering the two sensory clusters as fix factor (ns: not significant, $P > 0.05$).

	Range	Median	P
ethanol (%,v/v)	11.8–15.5	13.4	ns
pH	3.2–3.8	3.6	ns
volatile acidity ($g\ L^{-1}$ of acetic acid)	0.1–0.9	0.3	ns
titratable acidity ($g\ L^{-1}$ of tartaric acid)	3.9–6.5	5.2	ns
reducing sugars ($g\ L^{-1}$)	1.1–4.8	2.2	ns
malic acid ($g\ L^{-1}$)	0.0–0.6	0.0	ns
lactic acid ($g\ L^{-1}$)	0.3–1.9	0.9	ns
total polyphenol index (TPI) (au)	19–111	56	<0.05

3.2. Metabolomic analysis by UPLC − QTOF-MS

Unsupervised analysis revealed 14,280 and 6012 chemical features in ESI + and ESI − modes, respectively. PCA undertaken with the area of all features separately for ESI + and ESI − modes showed the pool of QC samples was projected in the middle of all samples in each case, thereby demonstrating the quality of the data (Fig. A.2 of Appendix A). Independent QC sample injections, performed throughout the analysis of sample batches, showed minimal variation and are plotted very close together, which confirms the reliability of the untargeted measurements undertaken at different times.

According to one-way ANOVA calculated with the sensory clusters as fixed factor, among the total of 20,292 features, significant differences were found for 1960 features for ESI+ (14 % of original features) and 410 for ESI− (6 % of original features). These were therefore considered as tentative markers possibly involved in the sensory differences among the wines studied.

The pattern of the selected features (i.e., their correct assignment to any of the two sensory groups) was visually inspected and confirmed one

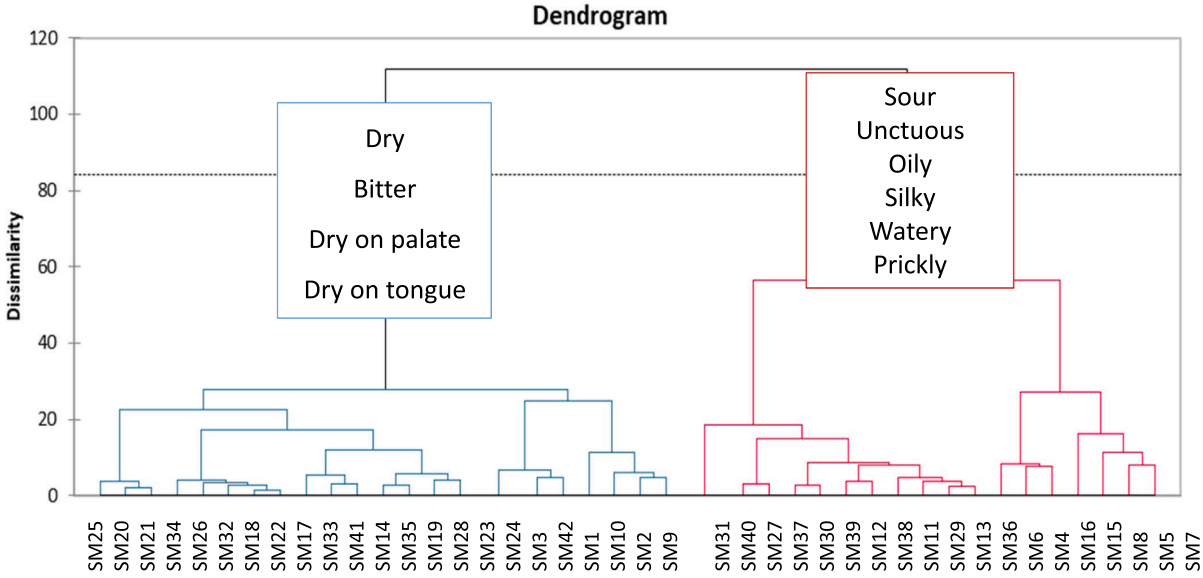

Fig. 2. HCA dendrogram of the 42 wines derived from the PCA calculated on the significant sensory descriptors scored following rate-k-attribute method. Attributes describing clusters refer to significant terms according to ANOVA analysis with cluster as fixed factor.

by one. Finally, Pearson correlation coefficients between sensory and semi-quantitative data were calculated to filter "putative markers". Accordingly, the final list of markers potentially involved in the taste and mouthfeel differences observed among wines was constituted by 36 tentative features from ESI + mode (Table A.5 of Appendix A) and 25 from ESI − mode (Table A.6 of Appendix A). Annotation was achieved for 26 in ESI + mode and 24 in ESI−, of which 19 were putatively annotated (i.e., second level annotation as defined in section 2.5.2) and 31 were putatively characterised (i.e., third level annotation).

Among the 61 features, 11 (18 %) belonged to the list of 108 compounds analysed by targeted analysis (Table A.3 of Appendix A). They include four pigment-related compounds (three pyranoanthocyanins and one malvidin-3-*O*-glucosyde-ethyl-flavan-3-ol derivative), three flavan-3-ol derivatives (epicatechin gallate, one dimeric and one trimeric procyanidin), three sulfonated flavan-3-ol derivatives (epicatechin-, epigallocatechin-, and a dimeric procyanidin type B sulfonate), and pantheteine sulfonate.

3.3. Relationship between chemical and sensory data

Using the peak area of compounds assigned from targeted (Table A.3 of Appendix A) and untargeted (Tables A.5 and A.6 Appendix A) analyses, five sensory variables out of 12 could be predicted by PLS regression (Table 2). This comprised three fully validated PLS models predicting sensory properties ("sour", "prickly", "dry") from targeted metabolites and another two ("oily", "unctuous") along with "dry" from untargeted chemical variables. This result confirms that untargeted approaches enrich targeted data by broadening the number of predicted dimensions, thereby confirming the hypothesis of the study.

These modelled sensory terms contributed to three out of the four significant independent and non-correlated sensory dimensions identified in Section 3.1. That is, the first dimension, mainly contributed by the terms "dry" (positively) and "unctuous" (negatively), the second dimension by "oily" (positively) and "sour" (negatively), and the fourth by "prickly" could be modelled. Differently, any of the terms defining the third dimension (mainly contributed by "sweet" and "burning") could not be suitably predicted, but sweetness of unoaked dry red wines is likely to be related to grape-derived compounds such as astilbins or *epi*-dihydrophaseic acid-3'-*O*-β-glucopyranoside (Cretin et al., 2019; Fayad et al., 2021). Regarding the "burning" sensation, it was not correlated to the level of ethanol but could be linked to the concerted effect of certain volatile compounds with reported chemesthesic properties, such as aldehydes and isoamyl alcohol (Arias-Pérez et al., 2021).

3.3.1. PLS models from targeted analysis

Of the 108 chemical features analysed, 76 contributed to the construction of the predictive models (Table 3). The explained variances from model calibration were 69 %–88 % (Table 2), corresponding to correlation coefficients between 0.83 and 0.94. Validated models explained at least 53 % of original variance (R^2) by cross-validation, which corresponds to high correlation coefficients (r) ranging from 0.73 to 0.81 (average = 0.76).

Regarding the "sour" attribute, which should correlate well with titratable acidity in red wines, there was a significant positive relationship ($F = 6.320$; $P = 0.016$), but only a modest correlation coefficient ($r = 0.37$). Instead, the perception of "sour" taste could be related to individual chemical compounds. The obtained model included 47 significant variables, having relatively low weighted regression coefficients that were mostly negative, including compounds related to drying such as most of the acids measured, flavan-3-ols, flavonols, and the bitter-like amino acid valine showing the largest negative coefficient in the model (−0.20). The exception among acids was indole-3-lactic acid hexoside sulfonate, which contributed to the model among the compounds with the highest positive coefficients (0.11) together with two sulfonated flavan-3-ols (epicatechin sulfonate, 0.11, and epigallocatechin sulfonate, 0.13), which were previously reported in wine (Arapitsas et al., 2016). However, the direct sensory relevance of such sulfonates has not been determined so far. Other compounds with positive regression coefficients were six anthocyanins and anthocyanin-derived pigments, gluthatione *S*-sulfonate, and the bitter-like tyrosine (Delompré et al., 2019; Yu et al., 2022) (Table 3). Considering that at least some are reported to be astringent and bitter, the relevance of these compounds to sour taste would appear to be indirect. This is supported by the negative and highly significant correlation between "sour" and the attributes "dry" ($r = -0.56$; $F = 18.58$; $P < 0.001$) and "bitter" ($r = -0.55$; $F = 17.59$; $P < 0.001$). This could be attributable to the ability of both sensations to modulate sour taste as a result of cognitive interactions related to attentional deviation. That is, the attention given to a specific attribute such as "sour" can present difficulties when other sensory properties are present at considerably higher perceived intensity (de-la-Fuente-Blanco et al., 2017). This is the case for "dry", that has a median intensity score of 2.2 (calculated from the 42 wines), which is 36 % higher than the median value for "sour" (median intensity score of 1.4).

Concerning the "prickly" attribute, it could be naïvely associated to higher total acidity ($r = -0.17$; $F = 1.169$; $P > 0.1$) and/or ethanol content ($r = -0.17$; $F = 1.311$, $P > 0.1$), but no significant correlations were observed. In contrast, a significant positive correlation was found for volatile acidity ($r = 0.57$; $F = 16.69$; $P < 0.001$). Besides this simple correlation, a validated PLS regression model was built with 23 out of the 108 compounds that were considered (Table 3). Phenolic compounds including ethyl coumarate (weighted regression coefficient = 0.16), malvidin-3-*O*-glucoside-vinylcatechol (0.16), epicatechin-malvidin-3-*O*-glucoside (0.15), coumaric acid (0.11), vanillic acid (0.11), and kaempferol-3-*O*-galactoside (0.11) mainly contributed positively to "prickly" sensation, as did most flavonols, cinnamic acid, ethyl caffeoate, and malvidin-3-*O*-glucoside-4-vinylphenol although to a lower extent. The direct role of vanillic and hydroxycinnamic acids on puckering mouthfeel and of caffeic and coumaric acid ethyl esters on astringent perception has previously been shown by sensory-directed experiments with red wines (Hufnagel & Hofmann, 2008; Sherman et al., 2020), which supports their capacity of modulating mouthfeel perception and thus helping to confirm the validity of the approach. Protocatechuic acid and its ethyl ester were reported to be involved in modulating wine mouthfeel in those studies, as observed in the present work with models showing a negative contribution of these compounds (weighted regression coefficients of − 0.15, and − 0.10, respectively) to the "prickly" sensation. Worthy of remark is the different effect caused by a variety of amino acids such as proline (−0.09), contributing negatively to the "prickly" model, and phenylalanine (0.09) and leucine (0.09) showing positive weighted regression coefficients. The role of proline on wine mouthfeel has been already reported in red wine models, where a masking effect was observed on astringency perception (Espinase Nandorfy et al., 2022). In contrast, phenylalanine and leucine

Table 2
Variables modelled by PLS regression, showing % of explained variance by cross-validation (Val), the number of latent variables (LV) included in each model, % of explained variance from calibration (Cal), and the root mean square error (RMSE) for cross-validation (RMSECV) and calibration (RMSEC).

variable	*% explained variance Val (LV) [Cal]*	*RMSECV [RMSEC]*[a]
Targeted approach		
sour	53 % (3) [74 %]	0.70 [0.54]
prickly	54 % (2) [69 %]	0.71 [0.54]
dry	66 % (4) [88 %]	0.58 [0.34]
Untargeted approach		
unctuous	55 % (4) [76 %]	0.68 [0.48]
oily	39 % (2) [60 %]	0.70 [0.60]
dry	74 % (3) [87 %]	0.48 [0.34]

[a] RMSE is given in z-units for a normal distribution. Given that 99.7 % of normal values are between z = − 3 and z = 3, an RMSE of 0.6 represents around 10 % of the range.

are reported to impart bitterness (Hufnagel & Hofmann, 2008), with their contribution to wine mouthfeel perception being unknown.

A validated PLS model was also obtained for "dry" from the targeted analytical method. It included four LVs and explained 88 % of the original variance by calibration, which corresponds to the highest correlation coefficient (r = 0.9; RMSEC = 0.34) observed among the three models derived from targeted analysis. The explained variance by cross-validation reached 66 % (correlation coefficient of 0.8) with a RMSECV of 0.58 (Table 2). The model was positively contributed by four flavan-3-ols, two flavonols, four acids and one of their corresponding

Table 3
Heatmap with weighted regression coefficients of variables included in the validated PLS models predicting "sour", "prickly" and "dry" from targeted chemical variables. Colour legend as follows:

0.23	0.13	0.03	0.00	−0.03	−0.13	−0.20

	SOUR	PRICKLY	DRY
FLAVAN-3-OLS			
gallocatechin		−0.05	0.05
epigallocatechin	−0.05		0.06
catechin			
epicatechin	−0.02		
procyanidin B3 dimer	−0.05		
procyanidin B1 dimer	−0.04		0.07
procyanidin B4 dimer	−0.06		
procyanidin B2 dimer	−0.04		
procyanidin B5 dimer	−0.04		
procyanidin type B trimer			0.1
procyanidin type B trimer	−0.04		
procyanidin type B trimer	−0.04		
FLAVONOLS AND DERIVATIVES			
myricetin-3-glucuronide	−0.13		0.18
myricetin-3-glucoside		0.07	
myricetin-3-rhamnoside	−0.09	0.08	−0.08
quercetin-3-galactoside	−0.06		
quercetin-3-glucuronide		−0.09	
quercetin-3-glucoside		0.06	−0.09
taxifolin		0.05	
kaempferol-3-galactoside		0.11	−0.07
kaempferol-3-glucuronide			−0.11
kaempferol-3-glucoside	−0.04		
syringetin			−0.1
syringetin-3-glucoside	−0.09		0.07
isorhamnetin	−0.03		
laricitrin	−0.03	0.09	
ACIDS AND DERIVATIVES			
shikimic acid	−0.1		0.12
gallic acid	−0.1		0.22
vanillic acid		0.11	
protocatechuic acid	−0.07	−0.15	
ethyl protocatechuate	−0.06	−0.1	−0.07
ethyl gallate	−0.13		0.22
caftaric acid	−0.05		
cis-coutaric acid			−0.12
fertaric acid	−0.06		−0.09
caffeic acid	−0.09		0.14
caffeic acid glucoside	−0.05		
ethyl caffeote	−0.09	0.08	
cinnamic acid		0.09	
coumaric acid	−0.08	0.11	0.09
coumaric acid glucoside	−0.11		
ethyl coumaric ester	−0.07	0.16	
ferulic acid			−0.1
tartaric acid		−0.1	−0.13
cis-aconitic acid	−0.05		

(*continued on next page*)

Table 3 (*continued*)

SULFONATE DERIVATIVES			
glutahione *S*-sulfonate	0.06		
tryptophol sulfonate			−0.06
indole-3-lactic acid glucoside		−0.11	
indole-3-lactic acid glucoside sulfonate	0.11		
epicatechin-4-sulfonate	0.11		−0.14
procyanidin B2-4-sulfonate			−0.14
epigallocatechin-4-sulfonate	0.13		
AMINO ACIDS			
proline		−0.09	−0.09
phenylalanine		0.09	
tyrosine	0.07		
valine	−0.2		0.23
leucine		0.09	
ANTHOCYANINS AND DERIVATIVES			
cyanidin-3-glucoside	0.06		−0.11
peonidin-3-glucoside			0.13
delphinidin-3-*O*-(6"-*p*-coumaroyl)-glucoside			−0.09
cyanidin-3-*O*-(6"-*p*-coumaroyl)-glucoside			−0.09
petunidin-3-*O*-(6"-*p*-coumaroyl)-glucoside			−0.09
peonidin-3-*O*-(6"-*p*-coumaroyl)-glucoside			0.07
malvidin-3-*O*-(6"-caffeoyl)-glucoside	0.06		−0.09
pyranomalvidin-3-*O*-(6"-acetyl)-glucoside	0.04		−0.07
pyranomalvidin-3-*O*-(6"-*p*-coumaroyl)-glucoside	0.04		
carboxypyranomalvidin-3-*O*-glucoside	−0.01		
carboxypyranopeonidin-3-*O*-glucoside	−0.06		0.23
carboxypyranopetunidin-3-*O*-glucoside	−0.07		0.11
carboxypyranomalvidin-3-*O*-(6"-acetyl)-glucoside	−0.02		
epicatechin-malvidin-3-*O*-glucoside		0.15	
epicatechin-ethyl-malvidin-3-*O*-glucoside	0.07		−0.06
malvidin-3-*O*-glucoside-4-vinylphenol		0.06	
malvidin-3-*O*-(6"-acetyl)-glucoside-4-vinylphenol			−0.06
malvidin-3-*O*-(6"-*p*-coumaroyl)-glucoside-4-vinylphenol	−0.02		
malvidin-3-*O*-glucoside-4-vinylcatechol	−0.1	0.16	

ethyl esters, one amino acid, and four anthocyanin-derived pigments. The highest weighted regression coefficients (Table 3) correspond to valine (0.23), carboxypyranopeonidin-3-*O*-glucoside (0.23), gallic acid (0.22), ethyl gallate (0.22), myricetin-3-*O*-glucuronide (0.18), caffeic acid (0.14), peonidin-3-*O*-glucoside (0.13), shikimic acid (0.12), carboxypyranopetunidin-3-*O*-glucoside (0.11), and a trimer of procyanidin B (0.10). The role played by flavan-3-ols, flavonols, caffeic acid, gallic acid, and ethyl gallate is well in accordance with previous sensory-directed experiments (Hufnagel & Hofmann, 2008), supporting the astringent-related character of these compounds. Regarding the contribution of peonidin and petunidin derivatives, it seems improbable that they are major drivers of drying, given their low concentrations in wine in comparison with other anthocyanin-derivatives. This may relate to an additive effect or them acting as markers of other chemical variables, but their true sensory role should be further confirmed. Concerning the amino acid valine, its involvement in the modulation of bitterness has been suggested (Delompré et al., 2019; Hufnagel & Hofmann, 2008). As with other components, its implication in wine drying sensations has not been reported and thus the sensory role of valine requires confirmation, such as via addition experiments.

Regarding the features negatively influencing the “dry” term, it is important to remark about the two sulfonated phenolic derivatives (procyanidin type B sulfonate and epicatechin 4-sulfonate), which present the largest negative regression coefficients in the targeted model (−0.14) (Table 3). The role of flavan-3-ol-sulfonate derivatives has been suggested to relate to a decline of astringency (i.e., drying in the present case) through the alteration of wine tannin profile (Ma et al., 2018), but their actual contribution to mouthfeel is unknown. Tartaric acid also appears to have an important negative influence on the model (−0.13), which could be attributed to a masking effect of sour taste elicited by this acid over dryness, as explained above. Also noteworthy are the negative weighted regression coefficients of major hydroxycinnamic acids (coutaric, ferulic and fertaric) and ethyl protocatechuate, which contrasts with previous work reporting a positive contribution of these compounds to the perception of astringency and puckering astringency of red wines (Hufnagel & Hofmann, 2008). Although publications confirm the contribution – either positive or negative – of these compounds to wine mouthfeel, the apparently conflicting results could be related to differences in the sensory protocol and thus in the sensory dimensions measured in the different works. On the other hand, the negative weighted regression coefficients of five out of the seven flavonols significantly contributing to the model for “dry” in the present work is potentially more in line with the velvety astringency attributed to this family of compounds (Hufnagel & Hofmann, 2008).

3.3.2. *PLS models from untargeted analysis*

The predictive model obtained for the “dry” attribute was higher than the model with targeted compounds using 3 LVs that explained 87 % of the original variance by calibration with an RMSEC of 0.34 (correlation coefficient of 0.9). The explained variance by cross-validation reached 74 %, corresponding to a correlation coefficient of 0.86, with RMSECV of 0.48. Among the 61 features considered, 30 were contributors to the model’s predictive ability for drying. A relative low number of variables (8 out of 30) contributed negatively to the model, with most having positive regression coefficients (Table 4). One trimer of procyanidin type B (0.23), the tripeptide Leu-Leu-Tyr (0.20), four anthocyanins

(regression coefficients ≥ 0.17) and one unknown compound (0.17; rt = 7.658; *m/z* (ESI −) = 743.1299) showed the highest positive weighted regression coefficients. The sensory role of both procyandins and anthocyanins to drying is supported by the literature (Ferrero-del-Teso et al., 2020; Hufnagel & Hofmann, 2008). This accorded with previous reports indicating that anthocyanins (likely containing other phenolic compounds) play a role in diverse mouthfeel properties such as "fullness" or traits including "dry", "roughness", and "chalky" (Vidal et al., 2004a), 2004b).

Notably, the involvement of peptides and proteins in tactile and astringent properties of aqueous solutions has been demonstrated (Solms, 1969). It has also been suggested that proteins are able to modulate astringent perception in red wine via interactions with polyphenols and polysaccharides to form ternary complexes (Le Bourvellec & Renard, 2012; Marassi et al., 2021), although their direct contribution to wine mouthfeel is still unknown. Regarding the compounds negatively contributing to the model, the moderating role of flavonols, hydroxycinnamic acids and malvidin-ethyl-flavan-3-ol derivatives on dryness is well in line the results derived from the model obtained from the targeted analysis. Despite the sensory role of anthocyanins, anthocyanin derivatives, and hydroxycinnamic acids in taste and mouthfeel perception of red wines being confirmed, the contribution to mouthfeel qualities of different chemical structures remains unknown.

Furthermore, the amino acid aminophenylalanine presents a discrete negative weighted regression coefficient (−0.06), suggesting a masking effect on "dry" akin to proline in the targeted model.

Along with "dry", another two sensory variables, "oily" and "unctuous", could be satisfactorily predicted from the untargeted approach (Table 4). Notably, "unctuous", which contributes negatively to PC1 (Fig. A.1a), presented a significant negative correlation with "dry" (r = − 0.42; F = 8.474; P < 0.01). This means that both terms belong to the same sensory dimension (i.e., when "dry" is high, "unctuous" is low and vice versa). A considerable number of features (28 out of 61, 46 %) presented relatively high weighted regression coefficients, indicating the effect that the studied chemical composition had on the "unctuous" attribute. Fourteen variables positively contributed to the model. Among them, one hydroxycinnamic acid derivative (regression coefficient = 0.36), two putatively characterised malvidin derivatives (0.31 and 0.26), one flavonol (0.25), and the sugar derivative ethyl glucuronide (0.17) presented the highest positive contributions to the model. Variables with the highest negative weighted regression coefficients in the "unctuous" model included anthocyanin-derivative compounds, flavan-3-ols, and one hydroxycinnamic acid, well in line with their positive contribution to the "dry" model (i.e., the opposite of "unctuous").

The PLS model obtained for "oily" included 2 LVs and explained 39 % of the original variance by cross-validation (r = 0.62) with a RMSECV of 0.70. Fifteen out of the 61 considered chemical variables contributed

Table 4
Heatmap with weighted regression coefficients of variables included in validated PLS-model predicting "unctuous", "oily" and "dry" mouthfeel from untargeted UPLC-QTOF-MS analysis using ESI+ (pos) and ESI− (neg) ionisation modes. Colour legend as follows:

0.36 | 0.26 | 0.16 | 0.00 | −0.10 | −0.20 | −0.31

RT	*m/z*	mode	group	annotation	unctuous	oily	dry
4.856	816.6379	pos	anthocyanin	malvidin-3-*O*-glucoside derivative			0.17
5.826	495.1114	neg	anthocyanin	carbinol pseudobase petunidin-3-*O*-glucoside derivative		0.09	
8.487	743.1284	neg	anthocyanin	delphinidin-3-*O*-(6"-*p*-coumaroyl)-glucoside-4-vinylcatechol	−0.04	−0.11	0.17
13.232	487.0894	neg	anthocyanin	pyranodelphinidin-3-*O*-glucoside	−0.07	−0.10	
15.834	503.1194	pos	anthocyanin	pyrano-petunidin-3-*O*-glucoside			0.05
15.837	501.1038	neg	anthocyanin	pyrano-petunidin-3-*O*-glucoside	−0.07		0.03
15.848	517.1043	pos	anthocyanin	carboxypyranocyaniding-3-*O*-glucoside			0.09
16.050	781.2002	pos	anthocyanin	malvidin-3-*O*-glucoside-(epi)catechin			0.08
17.739	517.1381	pos	anthocyanin	pyrano-malvidin-3-*O*-glucoside	0.26		
17.754	285.0761	pos	anthocyanin	anthocyanin derivative	−0.15		
18.331	635.1427	pos	anthocyanin	hydroxyphenyl-vinlylpyrano-malvidin-3-*O*-glucoside			0.03
18.790	224.0798	pos	anthocyanin	pyrano-malvidin-3-*O*-glucoside fragment	−0.25		0.21
19.341	807.2141	neg	anthocyanin	malvidin 3- *O*-glucoside-ethyl-(epi)catechin			−0.06
19.767	645.1615	neg	anthocyanin	malvidin-3-*O*-glucoside-ethyl-(epi)catechin fragment (correlation with 807.2141)		−0.14	−0.11
20.340	492.2789	pos	anthocyanin	malvidin-3-*O*-glucoside fragment of a malvidin-3-*O*-glucoside derivative	0.31		
17.350	795.2155	pos	anthocyanin-flavan-3-ol	petunidin-3-*O*-glucoside-ethyl-(epi)catechin	−0.27	−0.31	0.17
20.394	953.2556	neg	anthocyanin-flavan-3-ol	(epi)catechin-ethyl-malvidin-3-*O*-(6"-p-coumaroyl)-glucoside	0.11		
20.480	851.2428	pos	anthocyanin-flavan-3-ol	malvidin-3-*O*-(6"-*p*-coumaroyl)-glucoside-ethyl-catechin	−0.17		0.12
20.512	849.2264	neg	anthocyanin-flavan-3-ol	malvidin-3-*O*-(6"-acetyl)-glucoside-ethyl-(epi)catechin	0.09		
6.7610	729.2423	neg	flavan-3-ol	(epi)catechin-(4α->8)-(epi)gallocatechin gallate or (epi)gallocatechin-(4β->8)-(epi)catechin gallate adduct	−0.07		0.09
9.2490	867.2154	pos	flavan-3-ol	trimer procyanidin type B (catechin-catechin-catechin type)	−0.11		
9.2490	453.0852	pos	flavan-3-ol	procyanidin type B (trimer) fragment	−0.22		0.13
9.6720	865.1996	neg	flavan-3-ol	trimer procyanidin type B (catechin-catechin-catechin type)	−0.10		0.10
10.703	579.1532	pos	flavan-3-ol	procyanidin B2	0.12	−0.10	−0.16
10.758	577.1362	neg	flavan-3-ol	procyanidin B2			0.04
12.191	867.2161	pos	flavan-3-ol	trimer procyanidin type B (catechin-catechin-catechin type)			0.23
12.191	577.1346	pos	flavan-3-ol	procyanidin type B (trimer) fragment		0.09	
12.604	425.0878	neg	flavan-3-ol	procyanidin type B fragment			−0.05
17.726	441.0906	pos	flavan-3-ol	(epi)catechin gallate derivative fragment		0.25	0.09
3.806	385.0228	neg	sulfonated flavan-3-ol	epigallocatechin-4-sulfonate		−0.09	
7.067	369.0286	neg	sulfonated flavan-3-ol	procyanidin type B-4-sulfonate fragment	−0.15		
15.162	447.0942	neg	flavonol	kaempferol-3-*O*-glucoside derivative	0.25	0.19	−0.17
20.354	239.0259	pos	flavonol	kaempferol-3-*O*-glucuronide sodiate	0.14		−0.06
7.574	163.0753	neg	hydroxycinnamic acid	*trans*-*p*-coumaric acid derivative	−0.21		−0.14
8.501	258.992	neg	hydroxycinnamic acid	caffeic acid 3-*O*-sulfate or 3,5-dihydroxycinnamic acid sulfate	0.36		
4.279	613.1607	pos	tripeptide	glutathione disulfide (oxidised glutathione)	0.12		
6.198	181.0971	pos	amino acid	aminophenylalanine			−0.06
19.861	430.2304	pos	tripeptide	Leu-Leu-Tyr (leucyl-leucyl-tyrosine)		−0.14	0.20
4.969	300.0220	neg	sugar	*N*-acetyl-glucosamine phosphate	0.09	0.17	
3.638	221.0669	neg	sugar	ethyl glucuronide	0.17		
7.324	273.0542	pos		unknown	0.06		
7.658	743.1299	neg		unknown		−0.13	0.17
7.949	563.0933	pos		unknown	0.05	−0.05	0.07
12.351	299.0556	pos		unknown		−0.08	0.06
20.514	563.3161	pos		unknown	0.14		0.06
20.715	491.3198	pos		unknown	−0.20		0.05

to the "oily" model (Table 4), with most showing negative weighted regression coefficients. They include one anthocyanin-ethyl-flavan-3-ol, which had the greatest negative coefficient (−0.31), three anthocyanin derivatives (ranging from −0.10 to −0.14), one procyanidin (−0.10), and epigallocatechin-4-sulfonate (−0.09), as well as tripeptide Leu-Leu-Tyr (0.17) and three unknowns with $m/z = 743.1299$ (ESI −) (−0.13), $m/z = 563.0933$ (ESI +) (−0.05), and $m/z = 299.0556$ (ESI +) (−0.08). Among these, all except for epigallocatechin-4-sulfonate contributed positively to the "dry" model. In contrast, flavan-3-ol derivatives including an (*epi*)catechin gallate fragment (0.25), and a trimer of procyanidin type B (0.09), a flavonol (kaempferol 3-glucoside derivative, 0.19) and a sugar derivative (*N*-acetyl-glucosamine phosphate, 0.17) contributed positively to the "oily" model. The positive contribution of the flavan-3-ol fragments to the perception of "oily" cannot be explained without knowing the original molecule. Whereas the contribution of flavonols to wine mouthfeel and of sugars to sweet taste is known (Hufnagel & Hofmann, 2008), their role in "oily" perception remains unclear.

4. Conclusions

This study implemented a sensometabolomic strategy for characterising taste and mouthfeel properties of wine by combining multivariate data analysis of untargeted and targeted analytical outputs with sensory results obtained from a verbal sensory task (i.e., rate-k-attribute). A range of wine metabolites including polyphenols, pigments, acids, sulfonate, amino acids, and small peptides were related to diverse mouthfeel descriptors. The outcomes have demonstrated this to be a promising strategy for elucidating the chemical basis of taste and mouthfeel in wines by considering more than the usual metrics associated with tannin.

It is notable that only five out of the 12 significant sensory variables could be modelled, which related to three out of the four independent and non-correlated sensory dimensions identified by PCA in this work. It is therefore acknowledged that the chosen targeted and untargeted LC-MS approaches may still have limitations and that the continued development of analytical tools could be a key factor to more fully understand the taste and mouthfeel properties attributable to sensory-active compounds such as polysaccharides, peptides or proteins. Ultimately, developing methods to obtain information related to the structure of other macromolecules aside from polyphenols seems fundamental to fully understanding wine mouthfeel, but it remains a major challenge.

Overall, the results lay the foundation for testing of alternative hypotheses related to the taste and mouthfeel activity of different compounds in red wine. Investigation of orosensory properties and reconstitution studies are required to confirm the sensory role of the putative compounds, the relevance of their concentrations, and their chemical structures in the perception of red wine mouthfeel and taste.

CRediT authorship contribution statement

Sara Ferrero-del-Teso: Conceptualization, Investigation, Formal analysis, Writing – review & editing. **Panagiotis Arapitsas:** Conceptualization, Investigation, Writing – review & editing. **David W. Jeffery:** Conceptualization, Formal analysis, Validation, Writing – original draft, Writing – review & editing. **Chelo Ferreira:** Formal analysis, Writing – review & editing. **Fulvio Mattivi:** Writing – review & editing, Funding acquisition. **Purificación Fernández-Zurbano:** Writing – review & editing, Funding acquisition. **María-Pilar Sáenz-Navajas:** Conceptualization, Writing – review & editing, Writing – original draft, Funding acquisition, Visualization, Supervision.

Declaration of Competing Interest

The authors declare that they have no known competing financial interests or personal relationships that could have appeared to influence the work reported in this paper.

Data availability

Data will be made available on request.

Acknowledgements

This project was funded by the Spanish Ministry of Science and Innovation, the Spanish Research Agency and FEDER (projects: AGL-2017-87373-C3-3-R and PID2021-126031OB-C22 FEDER, UE). S.F.T acknowledges the University of La Rioja for her predoctoral fellowship (UR-CAR-2018). MPSN acknowledges the Spanish National Research Agency, the Ministry of Science, Innovation, and Universities and the European Social Fund for her postdoctoral fellowship: Ramón y Cajal Program (RYC2019-027995-I/AEI/10.13039/501100011033) and the Spanish Ministry of Universities funds of the Spanish Plan of Innovation, Technical and Scientific Research 2017–2020 – through the Jose Castillejo program (CAS21/00221). P.A., and F.M acknowledge the financial support from AdP 2019 funded by the Autonomous Province of Trento (Italy).

Appendix A. Supplementary material

Supplementary data to this article can be found online at https://doi.org/10.1016/j.foodchem.2023.137726.

References

Arapitsas, P., Speri, G., Angeli, A., Perenzoni, D., & Mattivi, F. (2014). The influence of storage on the "chemical age" of red wines. *Metabolomics, 10*(5), 816–832.

Arapitsas, P., Ugliano, M., Perenzoni, D., Angeli, A., Pangrazzi, P., & Mattivi, F. (2016). Wine metabolomics reveals new sulfonated products in bottled white wines, promoted by small amounts of oxygen. *Journal of Chromatography A, 1429*, 155–165.

Arias-Pérez, I., Sáenz-Navajas, M. P., de-la-Fuente-Blanco, A., Ferreira, V., & Escudero, A. (2021). Insights on the role of acetaldehyde and other aldehydes in the odour and tactile nasal perception of red wine. *Food Chemistry*, *361*, 130081.

Aydoğan, C. (2020). Recent advances and applications in LC-HRMS for food and plant natural products: A critical review. *Analytical and Bioanalytical Chemistry, 412*(9), 1973–1991.

Cevallos-Cevallos, J. M., & Reyes-De-Corcuera, J. I. (2012). Metabolomics in food science. *Advances in Food and Nutrition Research, 67*, 1–24.

Chávez-Márquez, A., Gardea, A. A., González-Rios, H., & Vazquez-Moreno, L. (2022). Characterization of Cabernet Sauvignon wines by untargeted HS-SPME GC-QTOF-MS. *Molecules, 27*(5).

Cretin, B. N., Waffo-Teguo, P., Dubourdieu, D., & Marchal, A. (2019). Taste-guided isolation of sweet-tasting compounds from grape seeds, structural elucidation and identification in wines. *Food Chemistry, 272*, 388–395.

de-la-Fuente-Blanco, A., Fernández-Zurbano, P., Valentin, D., Ferreira, V., & Sáenz-Navajas, M. P. (2017). Cross-modal interactions and effects of the level of expertise on the perception of bitterness and astringency of red wines. *Food Quality and Preference, 62*, 155-161.

Delompré, T., Guichard, E., Briand, L., & Salles, C. (2019). Taste perception of nutrients found in nutritional supplements: A review. *Nutrients, 11*(9).

Espinase Nandorfy, D., Watson, F., Likos, D., Siebert, T., Bindon, K., Kassara, S., Shellie, R., Keast, R., & Francis, I. L. (2022). Influence of amino acids, and their interaction with volatiles and polyphenols, on the sensory properties of red wine. *Australian Journal of Grape and Wine Research, 28*, 621–637.

Fayad, S., Le Scanff, M., Waffo-Teguo, P., & Marchal, A. (2021). Understanding sweetness of dry wines: First evidence of astilbin isomers in red wines and quantitation in a one-century range of vintages. *Food Chemistry, 352*, Article 129293.

Ferreira, V., San Juan, F., Escudero, A., Cullere, L., Fernandez-Zurbano, P., Saenz-Navajas, M. P., & Cacho, J. (2009). Modeling quality of premium Spanish red wines from gas chromatography-olfactometry data. *Journal of Agricultural and Food Chemistry, 57*(16), 7490–7498.

Ferrero-del-Teso, S., Suárez, A., Ferreira, C., Perenzoni, D., Arapitsas, P., Mattivi, F., Ferreira, V., Fernández-Zurbano, P., & Sáenz-Navajas, M. P. (2022). Modeling grape taste and mouthfeel from chemical composition. *Food Chemistry, 371*, Article 131168.

Ferrero-del-Teso, S., Suárez, A., Jeffery, D. W., Ferreira, V., Fernández-Zurbano, P., & Sáenz-Navajas, M. P. (2020). Sensory variability associated with anthocyanic and tannic fractions isolated from red wines. *Food Research International, 136*, Article 109340.

García-Estévez, I., Pérez-Gregorio, R., Soares, S., Mateus, N., & De Freitas, V. (2017). Oenological perspective of red wine astringency. *Oeno One, 51*(3), 237–249.

García-Estévez, I., Ramos-Pineda, A. M., & Escribano-Bailón, M. T. (2018). Interactions between wine phenolic compounds and human saliva in astringency perception. *Food and Function, 9*(3), 1294–1309.

Gawel, R., Oberholster, A., & Francis, I. L. (2000). A mouth-feel wheel: Terminology for communicating the mouth-feel characteristics of red wine. *Australian Journal of Grape and Wine Research, 6*, 203–207.

Gawel, R., Van Sluyter, S. C., Smith, P. A., & Waters, E. J. (2013). Effect of pH and alcohol on perception of phenolic character in white wine. *American Journal of Enology and Viticulture, 64*(4), 425–429.

Hufnagel, J. C., & Hofmann, T. (2008). Quantitative reconstruction of the nonvolatile sensometabolome of a red wine. *Journal of Agricultural and Food Chemistry, 56*(19), 9190–9199.

Jones, P. R., Gawel, R., Francis, I. L., & Waters, E. J. (2008). The influence of interactions between major white wine components on the aroma, flavour and texture of model white wine. *Food Quality and Preference, 19*(6), 596–607.

Kang, W., Niimi, J., Muhlack, R. A., Smith, P. A., & Bastian, S. E. P. (2019). Dynamic characterization of wine astringency profiles using modified progressive profiling. *Food Research International, 120*, 244–254.

Kueger, S., Steinhauser, D., Willmitzer, L., & Giavalisco, P. (2012). High-resolution plant metabolomics: From mass spectral features to metabolites and from whole-cell analysis to subcellular metabolite distributions. *The Plant Journal, 70*(1), 39–50.

Le Bourvellec, C., & Renard, C. M. (2012). Interactions between polyphenols and macromolecules: Quantification methods and mechanisms. *Critical Reviews in Food Science and Nutrition, 52*(3), 213–248.

Ma, W., Guo, A., Zhang, Y., Wang, H., Liu, Y., & Li, H. (2014). A review on astringency and bitterness perception of tannins in wine. *Trends in Food Science and Technology, 40*(1), 6–19.

Ma, L., Watrelot, A. A., Addison, B., & Waterhouse, A. L. (2018). Condensed tannin reacts with SO_2 during wine aging, yielding flavan-3-ol sulfonates. *Journal of Agricultural and Food Chemistry, 66*(35), 9259–9268. https://doi.org/10.1021/acs.jafc.8b01996

Marassi, V., Marangon, M., Zattoni, A., Vincenzi, S., Versari, A., Reschiglian, P., Roda, B., & Curioni, A. (2021). Characterization of red wine native colloids by asymmetrical flow field-flow fractionation with online multidetection. *Food Hydrocolloids, 110*, Article 106204.

Muñoz-Redondo, J. M., Puertas, B., Pereira-Caro, G., Ordóñez-Díaz, J. L., Ruiz-Moreno, M. J., Cantos-Villar, E., & Moreno-Rojas, J. M. (2021). A statistical workflow to evaluate the modulation of wine metabolome and its contribution to the sensory attributes. *Fermentation, 7*(2).

International Organisation of Vine and Wine, Compendium of International Methods of Wine and Must Analysis. OIV: Paris, France, 2021; Vol. 2.

Rinaldi, A., Vecchio, R., & Moio, L. (2021). Differences in astringency subqualities evaluated by consumers and trained assessors on Sangiovese wine using Check-All-That-Apply (CATA). *Foods, 10*(2), 218.

Sáenz-Navajas, M. P., Arias, I., Ferrero-del-Teso, S., Fernández-Zurbano, P., Escudero, A., & Ferreira, V. (2018). Chemo-sensory approach for the identification of chemical compounds driving green character in red wines. *Food Research International, 109*, 138–148.

Sáenz-Navajas, M. P., Avizcuri, J. M., Ferrero-del-Teso, S., Valentin, D., Ferreira, V., & Fernández-Zurbano, P. (2017). Chemo-sensory characterization of fractions driving different mouthfeel properties in red wines. *Food Research International, 94*, 54–64.

Sáenz-Navajas, M. P., Ferrero-del-Teso, S., Jeffery, D. W., Ferreira, V., & Fernández-Zurbano, P. (2020). Effect of aroma perception on taste and mouthfeel dimensions of red wines: Correlation of sensory and chemical measurements. *Food Research International, 131*.

Sherman, E., Coe, M., Grose, C., Martin, D., & Greenwood, D. R. (2020). Metabolomics approach to assess the relative contributions of the volatile and non-volatile composition to expert quality ratings of Pinot Noir wine quality. *Journal of Agricultural and Food Chemistry, 68*(47), 13380–13396.

Sumner, L. W., Amberg, A., Barrett, D., Beale, M. H., Beger, R., Daykin, C. A., … Viant, M. R. (2007). Proposed minimum reporting standards for chemical analysis. *Metabolomics, 3*(3), 211–221.

Toelstede, S., & Hofmann, T. (2008). Sensomics mapping and identification of the key bitter metabolites in Gouda cheese. *Journal of Agricultural and Food Chemistry, 56*(8), 2795–2804.

Vallverdú-Queralt, A., Meudec, E., Eder, M., Lamuela-Raventos, R. M., Sommerer, N., & Cheynier, V. (2017). The hidden face of wine polyphenol polymerization highlighted by high-resolution mass spectrometry. *ChemistryOpen, 6*(3), 336–339.

Vidal, S., Courcoux, P., Francis, L., Kwiatkowski, M., Gawel, R., Williams, P., Waters, E., & Cheynier, V. (2004). Use of an experimental design approach for evaluation of key wine components on mouth-feel perception. *Food Quality and Preference, 15*(3), 209–217.

Vidal, S., Francis, L., Noble, A., Kwiatkowski, M., Cheynier, V., & Waters, E. (2004). Taste and mouth-feel properties of different types of tannin-like polyphenolic compounds and anthocyanins in wine. *Analytica Chimica Acta, 513*(1), 57–65.

Wang, S., Olarte Mantilla, S. M., Smith, P. A., Stokes, J. R., & Smyth, H. E. (2021). Tribology and QCM-D approaches provide mechanistic insights into red wine mouthfeel, astringency sub-qualities and the role of saliva. *Food Hydrocolloids, 120*, Article 106918.

Yu, H., Wang, X., Xie, J., Ai, L., Chen, C., & Tian, H. (2022). Isolation and identification of bitter-tasting peptides in Shaoxing rice wine using ultra-performance liquid chromatography quadrupole time-of-flight mass spectrometry combined with taste orientation strategy. *Journal of Chromatography A, 1676*.